View metadata, citation and similar papers at core.ac.uk

brought to you by CORE

東北大学機関リポジトリ
TOUR
Tohoku University Repository

Microfabrication of microtip on photocantilever for near-field scanning microscopy and investigation of effect of microtip shape on spatial resolution

著者	桑野　博喜
journal or publication title	Journal of applied physics
volume	83
number	7
page range	3547-3551
year	1998
URL	http://hdl.handle.net/10097/35256

doi: 10.1063/1.366569

Microfabrication of microtip on photocantilever for near-field scanning microscopy and investigation of effect of microtip shape on spatial resolution

Yuriko Tanaka,[a] Kenji Fukuzawa, and Hiroki Kuwano
NTT Integrated Information and Energy Systems Laboratories, 3-9-11 Midori-cho, Musashino-shi, Tokyo 180, Japan

(Received 10 June 1997; accepted for publication 23 December 1997)

We experimentally investigated the dependence of spatial resolution on the shape of a microtip on our photocantilever, in order to improve the spatial resolution of near-field scanning optical microscopy. Two different cone angles of silicon-dioxide microtips were microfabricated by a new fabrication process. The experimental results, which indicate there is a relationship between the spatial resolution and cone angle of the microtip, were interpreted by calculations based on a simple theoretical model. © *1998 American Institute of Physics.* [S0021-8979(98)06307-5]

I. INTRODUCTION

Near-field scanning optical microscopy (NSOM) has made it possible to image optical-characteristic distributions with nanometer-order resolution beyond the diffraction limit.[1–3] NSOM based on localized total internal reflection (TIR) has been demonstrated by many groups.[4,5] In some types of this microscopy, an apertureless probe such as a microcantilever or a sharpened optical fiber is used.[6–8] The probe apex converts a nonpropagating evanescent light into a propagating light. The apex acts as a scattering center and the scattered light is then detected. In this apertureless NSOM with TIR, the spatial resolution is not limited by the smallness of the optical aperture. We have previously developed a ''photocantilever,'' which is an apertureless probe that can be used in NSOM based on TIR.[9,10] It is a microfabricated silicon cantilever with a *pn*-junction photodiode on its top. Figure 1 shows our NSOM concept using the photocantilever. It can simultaneously image a sample surface by NSOM and by atomic force microscopy (AFM).[11] We have also reported that the apex of the photocantilever converts evanescent light in the same way as in the other apertureless NSOMs.[12]

To get even higher spatial resolution, one must optimize the size, shape, and material of the probe apex that scatters the light. In this article, we report the fabrication of a microtip on the photocantilever as a well-defined scattering center and discuss the relationship between the resolution and the shape of the microtip, especially its cone angle. To improve the resolution, the volume of the scattering center must be small. A smaller cone angle is expected to produce higher lateral resolution like a smaller curvature radius does, although few reports have investigated the relationship between cone angle and resolution. However, a smaller cone angle will also reduce the intensity of the optical signal, that is, the scattered-light intensity, so the signal-to-noise ratio of the NSOM image will decrease. We investigated the optimum microtip cone angle to improve resolution, while maintaining sufficient optical signal intensity.

II. MICROFABRICATION PROCESS FOR MICROTIP ON PHOTOCANTILEVER

The microtip was fabricated in the process sequence shown in Fig. 2. In the usual fabrication of a microsharp cone by depositing material through a pinhole,[13,14] alkaline, or acid solvents must be used to completely remove the intermediate layer. However, those solvents would degrade the photodiode and aluminum electrodes of the photocantilever. We found a suitable combination of materials for fabricating the microtip on the photocantilever without degrading its components. This combination was a poly(methylmethacrylate) (PMMA)[15] layer as the intermediate layer and methylethylketone (MEK) as the solvent to remove layers.

The microfabrication for a photocantilever was described in previous papers.[9,10] We made the microtip just after the *pn*-junction photodiode and aluminum electrodes had been fabricated on the silicon wafer. The wafer was first coated with 1.0-μm-thick PMMA as an intermediate layer. Next, a 0.5-μm-thick aluminum layer was sputtered onto the PMMA layer, and a pinhole, which was 4 μm in diameter, was patterned in the aluminum layer with an acid etchant, an H_3PO_4/NH_4NO_3 mixture. An overhang structure was then produced by isotropic etching of the PMMA layer. The PMMA was etched with an O_2/CF_4 mixture gas, while the aluminum layer with a pinhole was used as a mask. When a SiO_2 layer was deposited with a thickness of approximately 10 μm at less than 100 °C by radio-frequency sputtering, a microtip was created from SiO_2 deposited through the pinhole. The wafer was then soaked in an organic solvent, MEK, to completely remove the layers other than the SiO_2 microtip from the wafer. The SiO_2 microtip had good adhesion to the substrate of the wafer, because it was deposited onto the oxidized silicon layer. After the microtip had been fabricated, the actual shape of the cantilever was created in the same way as described in previous papers.[9,10] To release the cantilever from the substrate, the front of the wafer was

[a]Electronic mail: yuriko@ilab.ntt.co.jp

 © 1998 American Institute of Physics

Downloaded 15 Oct 2008 to 130.34.135.158. Redistribution subject to AIP license or copyright; see http://jap.aip.org/jap/copyright.jsp

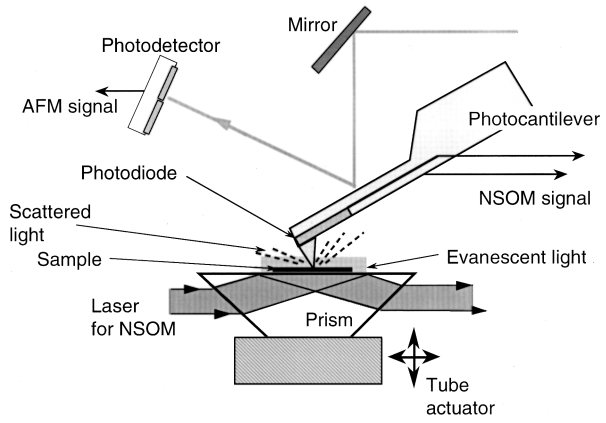

FIG. 1. Our NSOM concept. The sample is placed on a prism and illuminated with laser light at an angle that produces TIR. The apex of the photocantilever changes a non-propagating evanescent light into scattered light, which is collected by the photodiode to provide an optical signal for the NSOM.

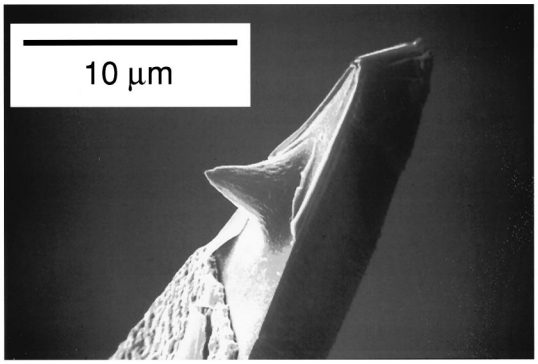

FIG. 3. SEM micrograph of the microtip on the end of the photocantilever.

next coated with polyimide. The wafer was then etched in an etchant (ethylene diamine pyrocatecoal, EDP) having an anisotropic nature, until the etch-stop layer was reached. Finally, the polyimide film was removed in an oxygen plasma, and the free-standing cantilever with the photodiode, aluminum electrodes, and microtip was completed. A scanning electron microscope (SEM) micrograph of a microtip on the end of the photocantilever is shown in Fig. 3. The fabricated microtip was approximately 2 μm high and its radius of curvature was about 50 nm as measured in an SEM micrograph at a higher magnification than that used to produce Fig. 3. Part of the aluminum electrodes can be seen at the bottom of the micrograph. Although a little polyimide also remained at the end of the cantilever, it did not degrade the NSOM/AFM imaging.

The microtip's height and curvature radius depended on the thickness of the intermediate PMMA layer as shown in Fig. 4. The diameter of the pinhole was constant (4 μm). The thinner the PMMA, the taller the microtip [Fig. 4(a)] and the smaller its curvature radius [Fig. 4(b)]. It was possible to control the height and radius of the microtip by altering the thickness of PMMA.

III. EXPERIMENT WITH DIFFERENT MICROTIP SHAPES

Two types of photocantilevers were used in NSOM/AFM imaging: one with a cone angle of 100°, and one with a cone angle of 50°. They were fabricated by the method described in Sec. II. The difference in the cone angle was made by varying the microtip's height. NSOM and AFM images were simultaneously observed by using these photocantilevers.

The experimental setup is shown in Fig. 5. The samples for imaging were (1) surfaces of indium-tin-oxide (ITO) thin film on a glass slide and (2) topographical mesas on an optical disk surface. They were both made of uniform material and had no distribution of different optical features at their surfaces, and had approximately 20-nm-high mesas. Index matching oil was added between the sample and the prism.

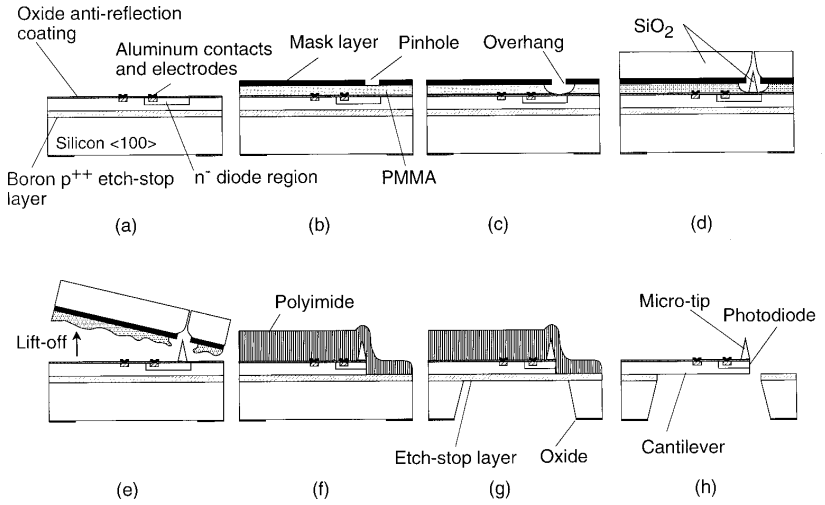

FIG. 2. Microfabrication sequence for a microtip on the photocantilever. (a) Creation of *pn* junction and the other components; (b) creation of PMMA intermediate layer and aluminum mask layer with a pinhole; (c) overhang creation by isotropic etching; (d) deposition of SiO_2 and microtip creation; (e) lift-off by MEK soaking; (f) cantilever patterning and polyimide coating; (g) substrate etching by ethylene diamine pyrocatecoal; (h) removal of polyimide coating.

Downloaded 15 Oct 2008 to 130.34.135.158. Redistribution subject to AIP license or copyright; see http://jap.aip.org/jap/copyright.jsp

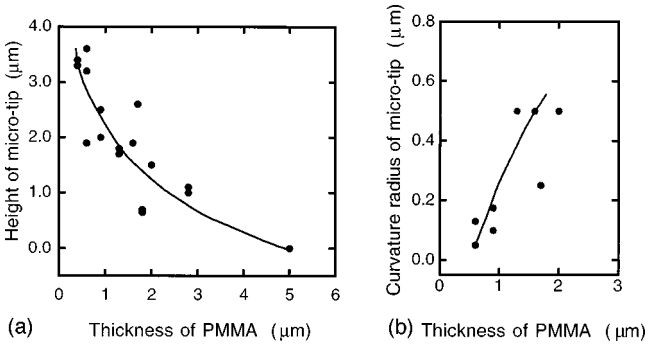

FIG. 4. Relationships between (a) microtip height and PMMA thickness, and (b) microtip curvature radius and PMMA thickness. The pinhole was 4 μm in diameter.

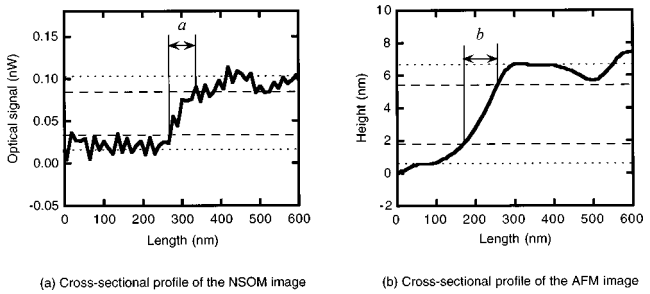

FIG. 6. Estimation of NSOM resolution from cross-sectional profiles of (a) NSOM and (b) AFM images. The sample was ITO thin film observed using a photocantilever with a microtip having a cone angle of 50°. The upper and lower levels of each slope are shown by the dotted lines, and the levels that determine ''*a*'' and ''*b*'' are shown by the dashed lines. The distance between the dashed lines is 60% of that between the dotted lines.

The laser was either a 5 mW He-Ne laser (λ=633 nm) or a 10 mW YAG laser (λ=532 nm) and illuminated the sample producing evanescent light. The evanescent light exists only close to the sample and is nonpropagating. Its intensity decays exponentially with increasing perpendicular distance z from the sample surface. The decay length d is the distance where the intensity is $1/e$ of that at the surface. The incident angle γ of the laser light was changed to vary the decay length of the evanescent light for each observation in this experiment shown in Fig. 5(a). As shown in Fig. 6, the cross-sectional profiles of the NSOM and AFM images of the ITO surface were obtained.

To discuss the spatial resolution of the NSOM, r_0 was defined in the following equation as a relative index, and was obtained by analyzing the cross-sectional profiles such as those shown in Fig. 6:

$$r_0=\frac{(a/b)}{(a'/b')}. \tag{1}$$

Here a/b expresses the ratio of the horizontal length of the slope in the cross-sectional profile by NSOM to that of the same slope by AFM, obtained using a photocantilever with a microtip. The levels that determine a and b are 20% inside the upper and lower levels of the slopes respectively as shown in Fig. 6. This ratio, in Eq. (1), is then normalized by a'/b', where a' and b' are the constant values of a and b respectively when the decay length d is 44.5 nm. Figure 7 plots the values of r_0 obtained from experimental measurements of a and b for various decay lengths for both cone angles as a parameter. The theoretical relationships are shown by the lines.

IV. INTERPRETATION OF THE EFFECT OF MICROTIP SHAPE

To interpret the experimental results, we calculated the relationship between spatial resolution and the cone angle using the model in Fig. 8. The microtip is approximated by a cone and the sample surface is assumed to be completely flat. The incident angle γ of the laser light to a sample is chosen to produce total internal reflection at the sample surface. In Fig. 8, p is the power density of the laser light spot and 2Θ is the cone angle of the microtip. The z axis is the symmetry axis of the cone and its origin is at the sample surface. The x axis is defined as one direction in the sample surface plane.

The optical signal is assumed to be provided by the total scattered light from the microtip surface. Moreover, the total scattered light intensity is assumed to be directly proportional to the total intensity of the evanescent light that illu-

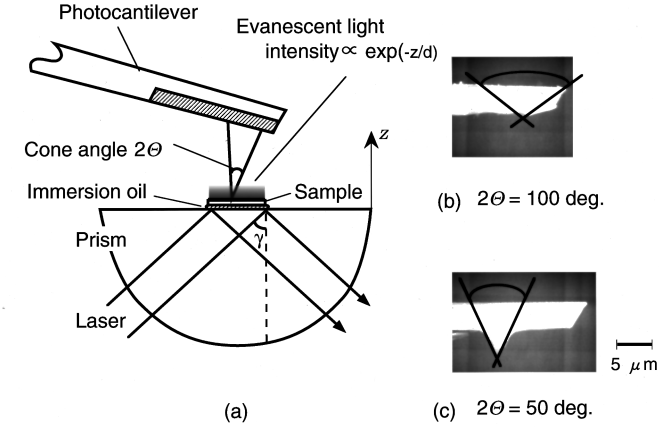

FIG. 5. (a) Experimental setup for investigating how the NSOM resolution depends on the cone angle of the microtip. The cone angles were (b) 100° and (c) 50°.

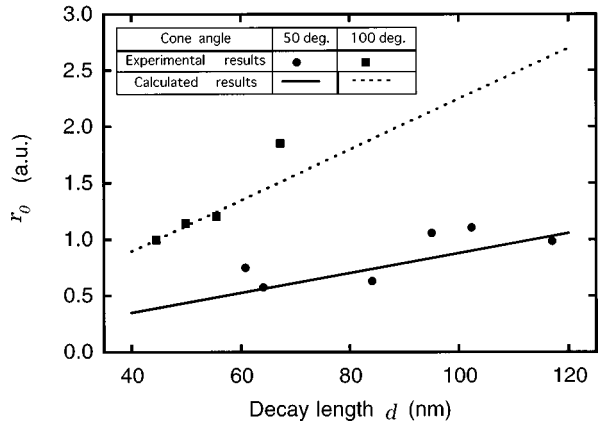

FIG. 7. Experimental results obtained using the photocantilever with the microtip. Calculated results are also shown.

Downloaded 15 Oct 2008 to 130.34.135.158. Redistribution subject to AIP license or copyright; see http://jap.aip.org/jap/copyright.jsp

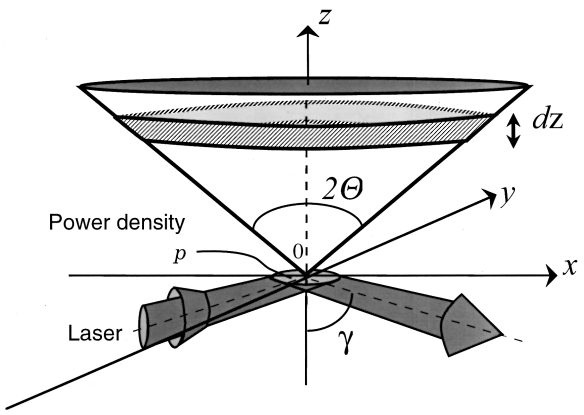

FIG. 8. Model for the calculation. The microtip is approximated by a cone. The axes are defined as shown here. The surface area of the cone is calculated by slicing it into narrow rings.

minates all of the cone's surface. The scattered light intensity from the surface of a narrow ring-shaped slice of the cone is expressed as

$$dI = 2\pi\alpha p \frac{\sin\Theta}{\cos^2\Theta} z \cdot \exp\left(-\frac{z}{d}\right) dz, \tag{2}$$

where d is the decay length of the evanescent light and α is a coefficient depending on the material of the microtip. The scattered light intensity from the surface area between 0 and z is thus given by

$$I(z) = \int_0^z dI. \tag{3}$$

The spatial resolution x_0 is defined as the length x providing an intensity that is 1/10 of the total scattered light. This value 1/10 is an arbitrary parameter in this calculation, and is chosen to clearly reveal any agreement between the experimental results and the calculated dependence of the resolution on the cone angle of the microtip. The ratio r_0 and the optical signal intensity I_t are given by

$$I_t = I(\infty) = 2\pi\alpha p \frac{\sin\Theta}{\cos^2\Theta} d^2, \tag{4}$$

$$\frac{I(z_0)}{I_t} = \frac{1}{10}, \tag{5}$$

$$r_0 = \frac{x_0}{x_0'} = \frac{z_0 \tan\Theta}{z_0' \tan\Theta} = \frac{z_0}{z_0'}, \tag{6}$$

where the intensity $I(z_0)$ that is 1/10 of the total scattered light is provided from a part of the cone surface ($z=0$ to z_0). The x_0 is the value of the spatial resolution, and r_0 is normalized by x_0'. The x_0' and z_0' are the spatial resolutions on condition that the decay length is 44.5 nm. I_t, in Eq. (4), is derived from Eqs. (2) and (3). In this study, we set $\alpha=1$ and $p=10^5$ (W/m^2).

In Fig. 7, the rough agreement between the experimental results and the calculated ones shows that this simple model is reasonable. Thus NSOM resolution is increased by using a photocantilever with a microtip having a small cone angle.

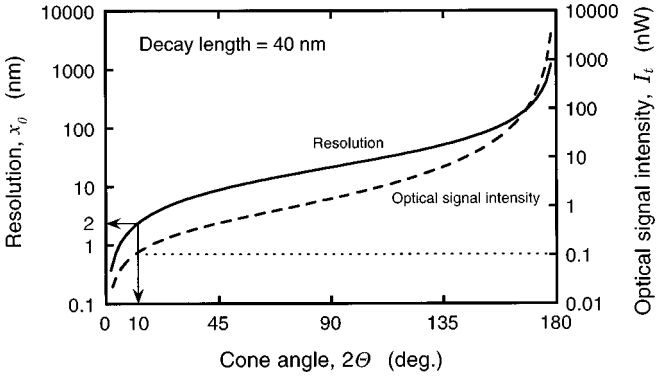

FIG. 9. Calculated relationships between the cone angle and the resolution, and between the cone angle and the optical signal intensity.

Moreover, we estimated the highest possible resolution of NSOM by calculating with the model. If the cone angle is small, the intensity of the total scattered light from the microtip becomes low. Namely, because this total scattered light is the optical signal being detected, the signal-to-noise ratio for an NSOM image depends on the cone angle. By calculating the optical signal intensity I_t from Eq. (4), we get the dependence of the optical signal intensity on the cone angle. Figure 9 shows the calculated relationship between the cone angle 2Θ and the spatial resolution x_0 or the optical signal intensity I_t for a decay length of 40 nm, which we usually used to obtain high resolution and sufficient intensity in our NSOM. This figure shows that the resolution becomes higher but the optical signal intensity decreases when the cone angle becomes smaller. Thus, we can calculate the optimum cone angle of the microtip that scatters enough intensity for the signal to be detected by the detector and apparatus. We estimate that an NSOM spatial resolution in the subnanometer range can be achieved by using an ideal high-efficiency photodiode and optimized cone angle of less than 10° in Fig. 9. However, because our current photodiode on the photocantilever can only detect light intensity of more than 0.1 nW, the cone angle must not be less than 10°, which gives the highest possible resolution as 2 nm.

V. CONCLUSION

We have microfabricated an SiO_2 microtip on the top of the photocantilever without degrading its photodiode and aluminum electrodes. In the experiment, the microtip with a smaller cone angle obtained a higher spatial resolution with the apertureless NSOM based on total internal reflection. We interpreted our experimental results using a simple calculation model. Considering the trade-off between the NSOM spatial resolution and the optical signal intensity, we conclude that subnanometer NSOM spatial resolution can be achieved using an ideal high-efficiency photodiode and a microtip with a cone angle of less than 10°.

ACKNOWLEDGMENTS

The authors thank Nobuhiko Kakuda, Kinya Kato, Keiichi Yanagisawa, and Yoshiaki Mimura for their support and stimulating discussions about the process of microfabrica-

Downloaded 15 Oct 2008 to 130.34.135.158. Redistribution subject to AIP license or copyright; see http://jap.aip.org/jap/copyright.jsp

tion. They also thank Takaya Tanabe for the sample preparation, and Satoko Nakano and Yasuo Kitahara for their support in fabricating and observing microtips.

[1] D. W. Pohl, W. Denk, and M. Lanz, Appl. Phys. Lett. **44**, 651 (1984).
[2] E. Betzig and J. K. Trautman, Science **257**, 189 (1992).
[3] F. Zenhausern, Y. Martin, and H. K. Wickramasinghe, Science **269**, 1083 (1995).
[4] D. Courjon, K. Sarayeddine, and M. Spajer, Opt. Commun. **71**, 23 (1989).
[5] M. Naya, S. Mononobe, R. U. Maheswari, T. Saiki, and M. Ohtsu, Opt. Commun. **124**, 9 (1996).
[6] R. C. Reddick, R. J. Warmack, and T. L. Ferrell, Phys. Rev. B **39**, 767 (1989).
[7] N. F. van Hulst, M. H. P. Moers, O. F. J. Noordman, R. G. Tack, F. B. Segerink, and B. Bölger, Appl. Phys. Lett. **62**, 461 (1993).
[8] Y. Inouye and S. Kawata, Opt. Lett. **19**, 159 (1994).
[9] S. Akamine, H. Kuwano, K. Fukuzawa, and H. Yamada, Proceedings of IEEE Workshop on Micro Electro Mechanical Systems, 1995, p. 145.
[10] S. Akamine, H. Kuwano, and H. Yamada, Appl. Phys. Lett. **68**, 579 (1996).
[11] K. Fukuzawa, Y. Tanaka, S. Akamine, H. Kuwano, and H. Yamada, J. Appl. Phys. **78**, 7376 (1995).
[12] K. Fukuzawa and H. Kuwano, J. Appl. Phys. **79**, 8174 (1996).
[13] T. R. Albrecht, S. Akamine, T. E. Carver, and C. F. Quate, J. Vac. Sci. Technol. A **8**, 3386 (1990).
[14] M. Hatzakis, J. Electrochem. Soc. **116**, 1033 (1969).
[15] H. N. Yu, R. H. Dennard, T. H. P. Chang, C. M. Osburn, V. Dilonardo, and H. E. Luhn, J. Vac. Sci. Technol. **12**, 1297 (1975).

Downloaded 15 Oct 2008 to 130.34.135.158. Redistribution subject to AIP license or copyright; see http://jap.aip.org/jap/copyright.jsp